The electron–electron instability in a spherical plasma structure with an intermediate double layer

V. Lapuerta and E. Ahedo
E.T.S.I. Aeronáuticos, Universidad Politécnica de Madrid, 28040 Madrid, Spain

(Received 11 December 2002; accepted 7 February 2003)

A linear dynamic model of a spherical plasma structure with an intermediate double layer is analyzed in the high-frequency range. The two ion populations tend to stay frozen in their stationary response and this prevents the displacement of the double layer. Different electron modes dominate the plasma dynamics in each quasineutral region. The electrostatic potential and the electron current are the magnitudes most perturbed. The structure develops a reactive electron–electron instability, which is made up of a countable family of eigenmodes. Space-charge effects must be included in the quasineutral regions to determine the eigenmode carrying the maximum growth rate. Except for very small Debye lengths, the fundamental eigenmode governs the instability. The growth rate for the higher harmonics approaches that of an infinite plasma. The instability modes develop mainly on the plasma at the high-potential side of the double layer. The influence of the parameters defining the stationary solution on the instability growth rate is investigated, and the parametric regions of stability are found. The comparison with a couple of experiments on plasma contactors is satisfactory. © *2003 American Institute of Physics.* [DOI: 10.1063/1.1564597]

I. INTRODUCTION

This paper studies the high-frequency perturbation modes developing in a spherical plasma structure consisting of two quasineutral plasmas separated by an intermediate, strong double layer (DL). A large potential drop takes place across the DL, which acts as a confining wall for one species from each plasma and as an acceleration layer for the other plasma species; therefore, each of the plasmas is constituted by two mildly disturbed species plus a high-velocity beam. In Refs. 1 and 2, we established a linear dynamic model for this three-region structure, based on a perturbation expansion of the complete steady-state solution. The stationary model had been formulated by Ahedo *et al.*[3] to study the plasma plumes created by electron-collecting plasma contactors.

As several review articles and proceedings books illustrate,[4–6] plasma structures with intermediate double layers are found in a variety of natural and laboratory phenomena and are the subject of many experimental, theoretical, and simulation studies. Experimental examples of these structures can be seen in Refs. 7 and 8 for contactor plumes, and in Refs. 9–11 for other laboratory plasmas. An important part of that research is devoted to the DL stability. The main experimental evidence is that DL structures can be sustained for long times, but, at the same time, large levels of plasma fluctuations of different frequencies are detected; in certain cases anomalous plasma heating is reported. Saturated current-driven instabilities seem the most probable cause of this behavior. However, there is a large controversy on which is, for each particular configuration, the dominant instability mode and its effect on the final state of the plasma. The cited review articles and the introductory section of Ref. 2 summarizes the varied conclusions of different research groups.

Numerical simulations are a usual way to approach the DL stability problem. Most of the simulations consider a finite, planar domain with two electrodes at the boundaries, each one acting as both plasma emitter and collector. Numerical results show, however, a large variety of behaviors: the DL can be (i) stable,[12] (ii) disrupted and rebuilt periodically,[12,13] or (iii) displaced toward the anode.[14,15] Hubbard and Joyce[12] point out that the most delicate issue is to impose correctly the boundary conditions, in order to avoid artificial wave reflection at the boundaries and coupling between plasma conditions at both electrodes. Part of the problem lies in the correct injection and collection of particles, which is not simple in counterstreaming plasmas.

In contrast to the simulation approach, our work follows a classical perturbation analysis of the three-region structure. The goals we try to achieve with this type of analysis are (i) to determine the main temporal modes developing at each side of the DL, (ii) to understand the interaction of the modes with the DL and the domain boundaries, (iii) to determine which instability types can develop around a DL structure, and (iv) to compare the response of this three-region structure with the results of the stability theory on homogeneous, infinite, multispecies plasmas (a problem we treated recently[16]). Of course, a linear analysis cannot predict the nonlinear behavior and eventual saturation of the instability, which are subjects more appropriate for a numerical simulation, but this approach presents its own issues, as we noted before. Our linear analyses can be helpful to deal with these issues.

Reference 2 showed that, because of the dissimilar characteristic times of response of ions and electrons, plasma equations and dynamics are rather different depending on the frequency range of the perturbation modes. That paper was devoted to the low frequency range, when electrons respond quasisteadily and ion-electron $(i-e)$ acoustic modes dominate the plasma response. A relevant feature then was the

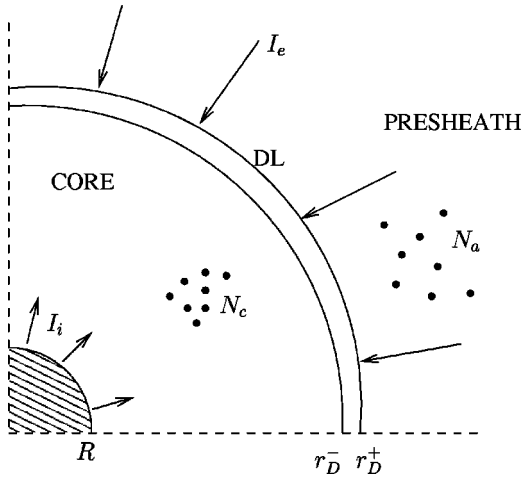

FIG. 1. Sketch of the spherical model with an intermediate DL.

coupling among the perturbation modes and the perturbation of the DL position (illustrated, in particular, by the Bohm and Langmuir conditions at the DL). And a key conclusion was that the plasma structure does not develop any (radial) reactive $i-e$ instability (that is, a Buneman-type instability); Ref. 16 reached the same conclusion for a simple plasma structure but using a more exact model, which included the Landau resonance.

The present work deals with the high-frequency range, when ions remain quasifrozen in their steady-state response and Langmuir and electron–electron ($e-e$) acoustic modes govern the plasma response. The general solution of the appropriate plasma equations is presented and several asymptotic limits are solved. For this frequency range, the development of a reactive $e-e$ instability in the high-potential, quasineutral region is expected.[16]

The paper is organized as follows. Section II formulates the complete unsteady model, presents briefly the steady-state solution, and derives the perturbation model. Sections III and IV analyze the perturbation responses in the low- and high-potential regions, and their matching through the DL. Section V comments regular responses to perturbed boundary conditions and Sec. VI discusses the $e-e$ instability modes. Section VII presents the main conclusions.

II. THE TIME-DEPENDENT MODEL

The model was formulated in Ref. 2 and Fig. 1 shows a sketch of it. The main features are summarized here. A spherical model is proposed, with r and t the radial and temporal variables. The contactor is a sphere of radius R immersed into a quiescent unmagnetized plasma (constituted by electrons e and ions a), of density N_∞ and temperature T_∞ in the region undisturbed by the contactor. This emits a second plasma (constituted by electrons c and ions i) and is biased to a positive potential, $\Phi_R(t)$, much larger than the mean plasma temperature. Ambient electrons are accelerated inwards and collected by the contactor; let $I_e(t)$ be the collected electron current. The emitted plasma is characterized by the current and temperature of emitted ions, $I_i(t)$ and T_{iR}, and the temperature T_c of emitted electrons, which remain confined around the contactor. The emission current $I_i(t)$ is assumed large enough for the plasma to sustain an intermediate DL; the region between the contactor and the DL is called the *core* and the external region is the *presheath*. The plasma Debye length, $\lambda_{D\infty}=(\epsilon_0 T_e/e^2 N_\infty)^{1/2}$, is assumed small enough to allow us a two-scale analysis and to treat the DL as a free discontinuity between two quasineutral plasmas.

A. Plasma equations

The dynamics of the four plasma species ($\alpha=i,e,a,c$) is given by the collisionless, macroscopic equations[2]

$$\frac{\partial N_\alpha}{\partial t}+\frac{1}{r^2}\frac{\partial J_\alpha}{\partial r}=0, \tag{1}$$

$$m_\alpha\frac{\partial V_\alpha}{\partial t}+\frac{\partial K_\alpha}{\partial r}=0, \tag{2}$$

$$T_\alpha N_\alpha^{1-\varrho_\alpha}=\text{const}, \tag{3}$$

with

$$J_\alpha=r^2 N_\alpha V_\alpha, \quad K_\alpha=m_\alpha V_\alpha^2/2+q_\alpha\Phi+H_\alpha. \tag{4}$$

Here, m_α is particle mass (we will take $m_a=m_i$), q_α is particle charge (all ions are assumed to be singly charged), N_α is density, T_α is temperature, V_α is macroscopic velocity, J_α is particle flow, K_α is mechanical energy, and ϱ_α is specific heat ratio. According to Ref. 3, we take $\varrho_\alpha=3$ for the free species, i and e, and $\varrho_\alpha=1$ for the confined species, a and c. Then, in Eq. (4), one has $H_\alpha=\varrho_\alpha T_\alpha/(\varrho_\alpha-1)$ for the free species and $H_\alpha=T_\alpha\ln N_\alpha$ for the confined species. The fluid equations are completed with Poisson equation for the electrostatic potential, $\Phi(r,t)$,

$$\frac{\varepsilon_0}{r^2}\frac{\partial}{\partial r}\left(r^2\frac{\partial\Phi}{\partial r}\right)=-\sum_\alpha q_\alpha N_\alpha. \tag{5}$$

In core and presheath, this equation simplifies into the quasineutral condition

$$\sum_\alpha q_\alpha N_\alpha=0.$$

In the thin double layer, the quasiplanar limit of the Poisson equation is used and the fluid equations become quasisteady in a reference frame tied to the DL. If $r_D(t)$ is the mobile position of the DL, which must be determined from the solution, Eqs. (1) and (2) yield

$$\begin{aligned} &J_\alpha-r_D^2 N_\alpha\, dr_D/dt\simeq\text{const},\\ &K_\alpha-m_\alpha V_\alpha\, dr_D/dt\simeq\text{const}. \end{aligned} \tag{6}$$

These conservation equations, valid within the DL, provide also jump conditions to match the quasineutral solutions at the two sides of the DL. The integration of the Poisson equation across the whole DL provides another jump condition,

$$S(\Phi_D^+)=S(\Phi_D^-), \tag{7}$$

where

$$S=\sum_{\alpha}\ (m_{\alpha}N_{\alpha}(V_{\alpha}-dr_D/dt)^2+N_{\alpha}T_{\alpha})$$

is the Sagdeev potential, and $\Phi_D^-(t)$ and $\Phi_D^+(t)$ are the potentials at the two DL sides. Equation (7) is known as the Langmuir condition and can be interpreted in two forms: (a) the total electric charge in the DL is zero; and (b) the stagnation pressure of the whole plasma is the same at the two DL sides. In addition, the Poisson equation provides the Bohm conditions for valid transitions between a non-neutral layer and a quasineutral plasma. For the present plasma configuration the Bohm condition at each side of the DL is[3]

$$S''(\Phi_D^+)=0, \quad S''(\Phi_D^-)>0. \tag{8}$$

Some simplifying assumptions can be made on the model, which facilitate the analytical treatment without modifying any central aspect of interest here. First, we assume a large potential jump through the DL, $\Phi_D^- - \Phi_D^+ \sim \Phi_R \gg T_\infty/e$, which allows us to neglect the densities N_c and N_i in the presheath, and N_a in the core. Second, the core size is assumed moderate [i.e., $r_D/R=O(1)$] in order to ignore thermal effects (due to spherical convergence) on the e beam in the core. And third, we take $T_{iR} \ll T_c$, which allows us to consider the species i as cold everywhere.

Variables are nondimensionalized with the help of R, N_∞, and T_∞. The main dimensionless variables are

$$\xi=\frac{r}{R}, \quad \phi=\frac{e\Phi}{T_\infty}, \quad t_\alpha=\frac{T_\alpha}{T_\infty}, \quad n_\alpha=\frac{N_\alpha}{N_\infty},$$
$$v_\alpha=\frac{V_\alpha}{(T_\infty/m_\alpha)^{1/2}}, \quad j_\alpha=\frac{J_\alpha}{R^2N_\infty(T_\infty/m_\alpha)^{1/2}}, \quad k_\alpha=\frac{K_\alpha}{T_\infty}. \tag{9}$$

The plasma/contactor model must determine the space–temporal response of the plasma for time-dependent conditions, $\Phi_R(t)$ and $I_i(t)$. In particular, the solution must yield the collected current $I_e(t)$, the position $r_D(t)$ of the DL, and the potentials at the two DL sides, $\Phi_D^-(t)$ and $\Phi_D^+(t)$. For time-dependent boundary conditions, a normal mode analysis is carried out. A generic variable, say f, is decomposed as the sum of a stationary part $f_0(r)$ and a time-dependent perturbation $f_1(r,t)$:

$$f(r,t)\simeq f_0(r)+f_1(r,t), \tag{10}$$

with $f_1(r,t)\propto\exp(-i\Omega t)$ and $\Omega=\Omega_{re}+i\Omega_{im}$ a complex frequency. In general, regular perturbation responses are studied for modes which are purely oscillatory in time, i.e., Ω real (and positive, unless otherwise is stated). On the contrary, in the stability analysis, eigenfrequencies have, in general, a nonzero imaginary part; $\Omega_{im}>0$ corresponds to unstable eigenmodes.

B. Stationary solution

This is denoted by subscript 0 and corresponds to the solution to stationary conditions at the contactor surface. Making $\partial/\partial t=0$ in Eqs. (1)–(3), the quasineutral plasmas verify $J_{\alpha 0}=$const and $K_{\alpha 0}=$const. Adding the quasineutral condition to these conservation equations, we have algebraic equations for the spatial profiles of the plasma magnitudes. These present turning (i.e., singular) points where

$$P_0\equiv S_0''=\sum_{\alpha}\frac{q_\alpha^2N_{\alpha 0}}{\varrho_\alpha T_{\alpha 0}-m_\alpha V_{\alpha 0}^2}=0, \tag{11}$$

which is the singular Bohm condition, Eq. (8); spatial derivatives become infinite at the turning points. The presheath/DL transition, $r=r_{D0}^+$, is one of them and the singularity on the electric field, $d\Phi_0/dr$, indicates the transition to the much thinner scale of the DL. On the contrary, the core/DL transition satisfies $P_0(r_{D0}^-)>0$. Then, one has $P_0(r)>0$ all along the core. Physically, the singularity at $r=r_{D0}^+$ means that the inward flow of population e enters the DL sonically (for a certain sound velocity), and the condition $P_0(r)>0$ for $R<r<r_{D0}^-$ means that the flow of population i is supersonic (for a certain sound velocity based on ion masses) in the core and at the core/DL transition. A second singular point appears at $r=R$: $P_0(R)=0$, meaning that the population i leaves the contactor sonically. Figure 2 shows an example of the stationary potential profile (in dimensionless variables).

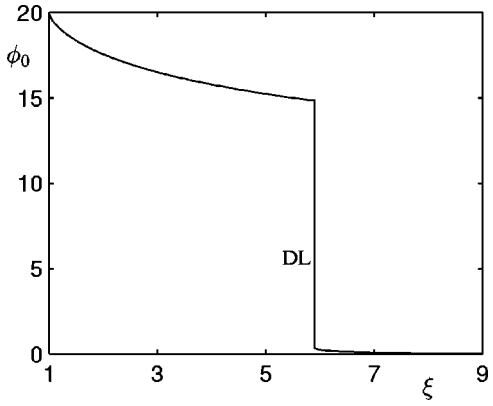

FIG. 2. Stationary solution. Profile of the electrostatic potential for $\phi_{0R}=20$, $\xi_{D0}=5.89$, and $t_{c0}=1$.

The stationary solution turns out to depend on three dimensionless parameters: the emitted current j_{i0}, the contactor potential ϕ_{0R}, and the temperature ratio t_{c0}. The collected current, $j_{e0}(j_{i0},\phi_{0R},t_{c0})$, increases with j_{i0}, ϕ_{0R} and t_{c0}^{-1}. The core size satisfies $\xi_{D0}\simeq 0.98\sqrt{|j_{e0}|}$. For convenience, we will use ξ_{D0} instead of j_{i0} as an input parameter. References 2 and 3 offer extensive details and results for the stationary solution.

C. Perturbation model

The perturbation equations for the particle flow and mechanical energy are, Eqs. (1)–(3),

$$dJ_{\alpha 1}/dr-i\Omega N_{\alpha 1}r^2=0, \tag{12}$$

$$dK_{\alpha 1}/dr-i\Omega m_\alpha V_{\alpha 1}=0, \tag{13}$$

where $N_{\alpha 1}$ and $V_{\alpha 1}$ are obtained from Eq. (4),

$$\frac{N_{\alpha 1}}{N_{\alpha 0}}=\frac{K_{\alpha 1}-q_\alpha\Phi_1-m_\alpha V_{\alpha 0}^2J_{\alpha 1}/J_{\alpha 0}}{\varrho_\alpha T_{\alpha 0}-m_\alpha V_{\alpha 0}^2},$$

$$\frac{V_{\alpha 1}}{V_{\alpha 0}}=\frac{-K_{\alpha 1}+q_\alpha \Phi_1-\varrho_\alpha T_{\alpha 0}J_{\alpha 1}/J_{\alpha 0}}{\varrho_\alpha T_{\alpha 0}-m_\alpha V_{\alpha 0}^2}. \tag{14}$$

Substituting $N_{\alpha 1}$ from Eq. (14) in the quasineutral condition $\Sigma q_\alpha N_{\alpha 1}=0$, the perturbed electric potential Φ_1 is expressed as a linear combination of $J_{\alpha 1}$ and $K_{\alpha 1}$,

$$\Phi_1=\frac{Q_1}{P_0},$$
$$Q_1=\sum_\alpha q_\alpha N_{\alpha 0}\frac{K_{\alpha 1}-m_\alpha V_{\alpha 0}^2 J_{\alpha 1}/J_{\alpha 0}}{\varrho_\alpha T_{\alpha 0}-m_\alpha V_{\alpha 0}^2}, \tag{15}$$

with P_0 as defined in Eq. (11).

The main boundary conditions for the perturbation problem in the core and the presheath are (i) the perturbation solution is continuous and bounded everywhere, (ii) the ambient plasma is unperturbed at $r=\infty$, and (iii) the perturbations on the emitted plasma variables at the contactor surface are specified. In addition, the core and the presheath must verify appropriate matching conditions at the DL.

Plasma perturbations produce a DL displacement, $r_{D1}(t)=r_D(t)-r_{D0}$, which affects the jump conditions of the perturbation problem. Taking into account this displacement, the total value of a generic variable $f(r,t)$ at the two quasineutral sides of the DL is given by

$$f(r_D^\pm,t)=f_0(r_D^\pm)+f_1(r_D^\pm,t)=f_0(r_{D0}^\pm)+\hat{f}_1(r_{D0}^\pm,t), \tag{16}$$

where

$$\hat{f}_1(r_{D0}^\pm,t)=f_1(r_{D0}^\pm,t)+r_{D1}\frac{df_0}{dr}(r_{D0}^\pm)$$

and higher-order terms have been neglected. From Eqs. (6), (7) and (16), the DL jump conditions of the perturbation problem are

$$[J_{\alpha 1}+i\Omega r_{D1}r_{D0}^2N_{\alpha 0}]_{r_{D0}^-}^{r_{D0}^+}=0, \tag{17}$$

$$[K_{\alpha 1}+i\Omega r_{D1}m_\alpha V_{\alpha 0}]_{r_{D0}^-}^{r_{D0}^+}=0, \tag{18}$$

$$\sum_\alpha \Big[2m_\alpha N_{\alpha 0}V_{\alpha 0}(V_{\alpha 1}+i\Omega r_{D1})+m_\alpha N_{\alpha 1}V_{\alpha 0}^2+\varrho_\alpha N_{\alpha 1}T_{\alpha 0}$$
$$+r_{D1}\frac{d}{dr}(m_\alpha N_{\alpha 0}V_{\alpha 0}^2+N_{\alpha 0}T_{\alpha 0})\Big]_{r_{D0}^-}^{r_{D0}^+}=0, \tag{19}$$

where $i\Omega r_{D1}$ is the DL displacement velocity and zeroth-order jump conditions have been applied already.

[In order to represent the perturbation response in Secs. V and VI, the spatial variable r needs to be stretched using a linear change $r\to s(r,t)$ described in Ref. 2, which transforms $r=R$ and $r=r_D(t)$ into $s=R$ and $s=r_{D0}$, respectively. Once solutions $f_0(r)$ and $f_1(r,t)$ are known, the total response of f at a given point, $s=s^*$ say, is $f(r(s^*,t),t)\simeq f_0(s^*)+\hat{f}_1(s^*,t)$. Equation (16) expresses that stretching at the DL boundaries.]

The dimensionless form of Eqs. (12) and (13) is

$$\frac{1}{\xi^2}\frac{dj_{\alpha 1}}{d\xi}-i\omega_\alpha n_{\alpha 1}=0, \tag{20}$$

$$\frac{dk_{\alpha 1}}{d\xi}-i\omega_\alpha v_{\alpha 1}=0, \tag{21}$$

where

$$\omega_\alpha=\Omega R(T_\infty/m_\alpha)^{-1/2} \tag{22}$$

are dimensionless frequencies based in each species mass. One has $\omega_i=\omega_e\sqrt{m_e/m_i}$ and because of the dissimilar masses of ions and electrons, there are two distinguished ranges, at least, for the frequencies of the perturbation modes:

(i) the *low frequency range* with $\Omega\sim R^{-1}\sqrt{T_\infty/m_i}$, yielding $\omega_i=0(1)$ and $\omega_e\ll 1$;

(ii) the *high frequency range* with $\Omega\sim R^{-1}\sqrt{T_\infty/m_e}$, yielding $\omega_e\gg 1$ and $\omega_e=0(1)$.

For a given frequency Ω, there are ion–electron $(i-e)$ modes of short wavelength, $\lambda\sim\Omega^{-1}\sqrt{T_\infty/m_i}$ and electron–electron $(e-e)$ modes of long wavelength, $\lambda\sim\Omega^{-1}\sqrt{T_\infty/m_e}$. Within the low frequency range, studied in Ref. 2, electrons behave quasisteadily and the response is governed by the $i-e$ modes. The problem can be studied taking $\omega_e\to 0$ in the equations, which means to consider infinite the wavelength of the $e-e$ modes.

Next sections of this paper deal with the high frequency range, where the ion populations tend to remain frozen (or rigid) in their stationary solution and the plasma response is governed by the $e-e$ modes. In each region, we will start analyzing the solution for the general case of both ω_e and ω_i finite. Then we will look for the asymptotic solution for $\omega_i=\infty$, when the wavelength of the $i-e$ modes tends to zero, implying, in general, a zero amplitude of these modes. The limit $\omega_i=\infty$ simplifies the ion equations but some boundary conditions cannot be satisfied unless some perturbation layers are added; these layers are determined from the analysis of the finite ω_i case.

Both $i-e$ and $e-e$ modes are quasineutral types of modes in core and presheath. In the high-frequency range, the presence of an $e-e$ instability introduces eigenmodes of a third type: non-neutral Langmuir modes of wavelength $\lambda\sim\lambda_d(R\Omega)^{-1}\sqrt{T_\infty/m_e}$. These modes play a central role in bounding the macroscopic $e-e$ instability[17] but require to formulate a non-neutral perturbation problem in presheath and core. An approximate treatment of this problem is presented in Sec. VI A.

III. PRESHEATH SOLUTION

A. General case: ω_i finite

In the presheath, the quasineutrality condition reduces to $n_a=n_e$, and species i and c can be ignored when we determine the potential profile. Then, the dimensionless problem reduces to

$$\phi_1=\frac{q_1}{p_0}=\frac{v_{e0}^2j_{e1}/j_{e0}-k_{e1}-(v_{e0}^2-3t_{e0})k_{a1}}{1+3t_{e0}-v_{e0}^2}, \tag{23}$$

for the electrostatic potential [with p_0 and q_1 the dimensionless counterparts of the capital case variables in Eqs. (11) and (15)] and four equations differential [Eqs. (20) and (21) for $\alpha=a,e$] with

$$\frac{n_{e1}}{n_{e0}}=\frac{k_{a1}+k_{e1}-v_{e0}^2 j_{e1}/j_{e0}}{1+3t_{e0}-v_{e0}^2},$$
$$\frac{v_{e1}}{v_{e0}}=\frac{(1+3t_{e0})j_{e1}/j_{e0}-k_{a1}-k_{e1}}{1+3t_{e0}-v_{e0}^2}, \tag{24}$$

$n_{a1}=n_{e1}$ and $v_{a1}=v_{e0}j_{a1}/j_{e0}$.

The general solution of the presheath is a linear combination of four modes, proportional to $\exp(-i\Omega t)$ (usually we omit to write this temporal dependence). Taking $\phi_1(\infty)=0$ and neglecting modes traveling inwards the asymptotic solution for $\omega_i\xi_{D0}\gg 1$ (justified in the following section) is

$$\phi_1\simeq j_{1\infty}\left(\frac{j_{e0}}{4\xi^4}-\frac{i\omega_e}{\xi}\right)+\frac{3a_\infty}{4\xi}\exp\left(\frac{i\omega_i}{2}\xi\right),$$
$$j_{a1}\simeq j_{1\infty}\left(\frac{4ij_{e0}}{\omega_i\xi^2}+\sqrt{\frac{m_e}{m_i}}\right)+\frac{a_\infty\xi}{2}\exp\left(\frac{i\omega_i}{2}\xi\right), \tag{25}$$
$$j_{e1}\simeq j_{a1}\sqrt{m_e/m_i}+j_{1\infty},$$

where a_∞ and $j_{1\infty}$ are constant; $-j_{1\infty}$ is the net perturbation current crossing the presheath and reaching $r=\infty$. The limit $m_e/m_i\to 0$ (i.e. $\omega_e\to 0$) in Eqs. (25) recovers the ion modes discussed in Ref. 2.

Two boundary conditions are imposed at the presheath/DL boundary,[2] which is characterized by $p_{0D}^+=0$, that is

$$v_{e0D}^+=-\sqrt{1+3t_{e0D}^+}\simeq -1.545, \tag{26}$$

the last number being obtained from the universal solution for the presheath. First, since the DL is a barrier for the ambient ions, their relative velocity there is zero,

$$[j_{a1}/\xi^2 n_{e0}]_{\xi_{D0}^+}+i\omega_i\xi_{D1}=0. \tag{27}$$

Second, the solution must be bounded at ξ_D^+. From Eqs. (16) and (23), the total perturbation of the electric potential at the DL boundary is

$$\hat{\phi}_{1D}^+\simeq\left[\frac{v_{e0}^2(j_{e1}/j_{e0}-2\xi_{D1}/\xi_{D0})-k_{e1}-(v_{e0}^2-3t_{e0})k_{a1}}{1+3t_{e0}-v_{e0}^2}\right]_{\xi_{D0}^+}, \tag{28}$$

which is bounded if

$$[(j_{e1}/j_{e0}-2\xi_{D1}/\xi_{D0})v_{e0}^2-k_{a1}-k_{e1}]_{\xi_{D0}^+}=0. \tag{29}$$

This condition is the Bohm singular condition of the perturbation problem for the electron modes. Solving the indeterminacy in Eq. (28), we have

$$\hat{\phi}_{1D}^+=\left[\frac{2v_{e0}^2(v_{e0}^2-1)}{2v_{e0}^2-1}\left(\frac{j_{e1}}{j_{e0}}-2\frac{\xi_{D1}}{\xi_{D0}}\right)-\frac{i\omega_e\xi_{D1}v_{e0}}{2v_{e0}^2-1}-k_{e1}\right]_{\xi_{D0}^+}.$$

For each ω_e mode the presheath solution depends on three parameters: ξ_{D1}, $j_{1\infty}$, and a_∞. Conditions (27)–(29), combined with the integration of Eqs. (20)–(21) and the asymptotic solution (25), leave only one of them free. We write

$$[j_{1\infty}\ \ a_\infty]A'=B'\xi_{D1}/\xi_{D0}, \tag{30}$$

for certain matrices A' and B', which depend on ω_e and the zeroth-order solution. As in Ref. 2, the numerical integration presents difficulties with the singularity at $\xi=\xi_{D0}^+$ and the unbounded mode traveling inwards from $\xi=\infty$. It is found that A' is a regular matrix for any ω_e; thus Eq. (30) provides, for each ω_e, the ratios $j_{1\infty}/\xi_{D1}$ and a_∞/ξ_{D1}.

B. Case $|\omega_i\xi_{D0}|\gg 1$

For this asymptotic case the presheath solution can be expressed as the combination of the WKB solution of the homogeneous problem plus a particular solution proportional to $j_{1\infty}$,[2,18]

$$j_{a1}(\xi)\simeq\tilde{a}_\infty\alpha_p(\xi)\exp[-\beta_p(\xi)]+j_{1\infty}\left(\frac{4iv_{e0}}{\omega_i\xi}\frac{1+3t_{e0}}{1+3t_{e0}-v_{e0}^2}-\sqrt{\frac{m_e}{m_i}}\right), \tag{31}$$

with $\tilde{a}_\infty$ a constant, $\alpha_p(\xi)$ defined in Ref. 2, and

$$\beta_p(\xi)=-i\omega_i\left[\int_{\xi_{D0}^+}^{\xi}(1+3t_{e0}-v_{e0}^2)^{-1/2}d\xi-\sqrt{m_e/m_i}\int_{\xi_{D0}^+}^{\xi}v_{e0}(1+3t_{e0}-v_{e0}^2)^{-1}d\xi\right].$$

These equations show that the perturbations in the presheath consist of a stationary mode and an $i-e$ mode traveling outwards with (dimensionless) group velocity $(1+3t_{e0}-v_{e0}^2)^{1/2}$. The transition from the low to the high frequency range is illustrated by the terms with $\sqrt{m_e/m_i}$, which are negligible for $\omega_i=O(1)$ but dominant for $\omega_i\to\infty$. The asymptotic solution (25) for $|\omega_i\xi|\gg 1$ comes out from Eq. (31).

The WKB solution becomes singular at the presheath/DL boundary, where Eq. (26) is satisfied. For $\xi/\xi_{D0}-1\ll 1$ and $\mathrm{Im}(\omega_e)\neq 0$, the solution matching with Eq. (31) is

$$j_{a1}(\xi)\simeq 2i\tilde{a}_\infty c_1\,\mathrm{Ai}(z)-j_{1\infty}c_2\,\mathrm{Gi}(z), \tag{32}$$

where

$$z(\xi)=(2\omega_i\xi_{D0})^{2/3}a_0^{-1/3}(\xi/\xi_{D0}-1)^{1/2},$$

Ai, Bi, Gi, and Hi are Airy functions and a_0, c_1, c_2 are constants defined in Ref. 2; the solution for $\mathrm{Im}(\omega_e)=0$ presents a similar form.[2]

The boundary conditions (27)–(29) at $\xi=\xi_{D0}^+$ relate $\tilde{a}_\infty$ and $j_{1\infty}$ to ξ_{D1}. Keeping only the dominant terms for $|\omega_i\xi_{D0}|\gg 1$ and substituting known quantities, one has

$$\frac{|j_{1\infty}|}{|j_{e0}|}\simeq 0.372(|\omega_i|\xi_{D0})^{4/3}\frac{|\xi_{D1}|}{\xi_{D0}}\propto|\omega_i|^{4/3}|\xi_{D1}|, \tag{33}$$

$$\frac{|\tilde{a}_\infty|}{|j_{e0}|}\simeq 0.528|c_3|(|\omega_i|\xi_{D0})^{5/6}\frac{|\xi_{D1}|}{\xi_{D0}}, \tag{34}$$

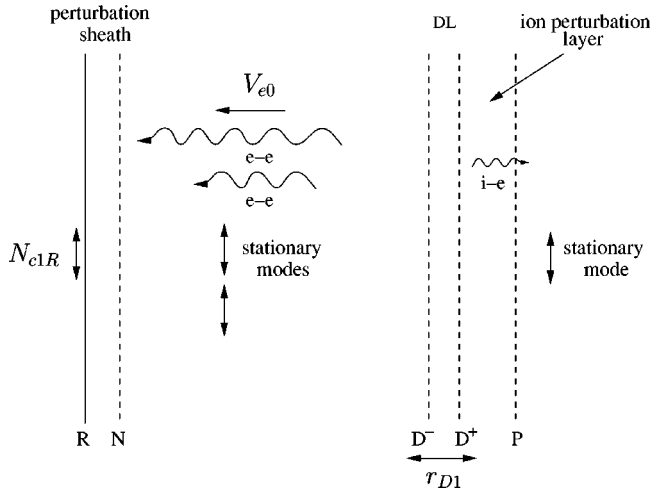

FIG. 3. Sketch of the different plasma regions and perturbation modes in the high-frequency range.

with $|c_3|$ equal to 1 and 2 for $\mathrm{Im}(\omega_e)\neq 0$ and $\mathrm{Im}(\omega_e)=0$, respectively.

C. Case $|\omega_i \xi_{D0}|=\infty$

For $\omega_i \to \infty$, Eq. (33) shows that $\xi_{D1} \sim \omega_i^{-4/3} \to 0$ must be satisfied for $j_{1\infty}$ to be finite. Then, Eq. (34) yields $\tilde{a}_\infty \propto \omega_i^{-1/2} \to 0$. Therefore, at high frequencies, the $i-e$ modes and the DL displacement become negligible; indeed, condition (27) shows that the second effect is the consequence of the first one. It is noteworthy that, for $\omega_i \to \infty$, finite perturbations of electron current, $j_{1\infty}$, are compatible with $\xi_{D1} \to 0$. Setting $n_{a1}=n_{e1}=0$ and $j_{a1}=0$, the presheath solution satisfies

$$j_{e1}=j_{1\infty}, \quad k_{e1}=i\omega_e j_{1\infty}\int_\infty^\xi \frac{d\xi}{\xi^2 n_{e0}},$$
$$\phi_1=k_{a1}=-k_{e1}+\frac{v_{e0}^2}{j_{e0}}j_{1\infty}. \tag{35}$$

However, this solution is not valid for $\xi \to \xi_{D0}^+$, because the density perturbation of the plasma density at the DL boundary is not zero: from Eq. (24) one has

$$\frac{\hat{n}_{e1D}^+}{\hat{n}_{e0D}^+}=\frac{(v_{e0D}^+)^2}{2(v_{e0D}^+)^2-1}\frac{j_{1\infty}}{j_{e0}} \simeq 0.63\frac{j_{1\infty}}{j_{e0}} \neq 0. \tag{36}$$

Therefore, a boundary layer with nonzero ion perturbations (region PD^+ in Fig. 3) must exist close to the DL outer boundary. There, j_{a1} satisfies Eq. (32) [for $\mathrm{Im}(\omega_e)\neq 0$] yielding

$$\frac{\hat{n}_{e1}(z)}{n_{e0}} \simeq -\frac{(a_0 i\omega_i \xi_{D0})^{2/3}}{2\,\mathrm{Ai}(0)(1+3t_{e0}-v_{e0}^2)}\frac{\xi_{D1}}{\xi_{D0}} \times (\mathrm{Ai}'(z)+\sqrt{3}\mathrm{Gi}'(z)),$$

and $\hat{n}_{e1}(z=0)$ satisfies Eq. (36). Setting $z \sim O(1)$ in this solution, the characteristic thickness of this layer is $\Delta\xi \sim \xi_{D0}|\omega_i \xi_{D0}|^{-4/3}$. From Eqs. (20) and (21), j_{e1} and k_{e1} are clearly constant across this layer. With respect to the variations of ion magnitudes, we find $\Delta j_{a1} \sim \omega_i^{-1/3}$ and $\Delta\phi_1 \simeq \Delta k_{a1} \sim \omega_i^{-2/3}$, so these variations can be neglected too. Then, Eqs. (35) yield

$$j_{e1D}^+ \simeq j_{1\infty}, \quad k_{e1D}^+ \simeq c_p i\omega_e j_{1\infty}, \quad \phi_{1D}^+ \simeq -k_{e1D}^+ + c_p' j_{1\infty}, \tag{37}$$

with $c_p=1.1\xi_{D0}/j_{e0}$ and $c_p'=2.4/j_{e0}$. These expressions relate the magnitudes at the DL external boundary to $j_{1\infty}$ and will be used in Sec. IV to continue the integration of the perturbation problem in the core.

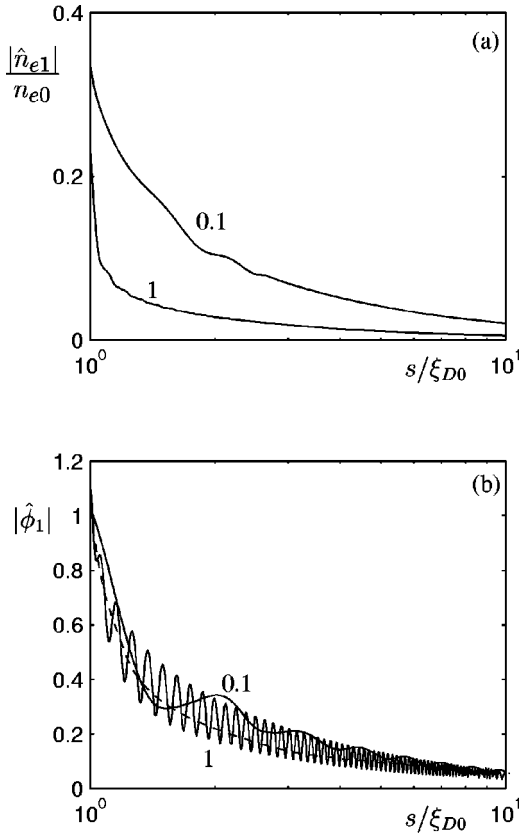

FIG. 4. Presheath. Envelope of the spatial response to perturbations of frequency $\omega_e \xi_{D0}=0.1$ and 1; amplitudes are normalized with $|\hat{\phi}_{1D}^+|=1$. The mass ratio is $\sqrt{m_e/m_i}=0.01$. The dashed line in (b) corresponds to the asymptotic solution for $\omega_i=\infty$.

D. Results

Figure 4 shows the temporal envelope of the spatial perturbations on $\hat{n}_{e1}$ and $\hat{\phi}_1$ for different values of ω_i, obtained from the numerical integration of the differential equations. As predicted above, the density perturbations tend to be confined near the DL as $|\omega_i|$ grows. The asymptotic solution for $\omega_i=\infty$, Eq. (35), has been included in Fig. 4(b). It recovers very well the average behavior of $\hat{\phi}_1$ but not, of course, the small, short-wavelength, ion–electron mode.

IV. CORE SOLUTION AND PROBLEM CLOSURE

A. General case: ω_i finite

The quasineutrality condition in the core reduces to $n_{e1}+n_{c1}=n_{i1}$, and the species a can be ignored to determine the potential profile. The core problem consists of the differ-

ential equations (20) and (21), for $\alpha=e,c,i$, plus the quasineutrality condition. Operating conveniently with the continuity equations, one of the differential equations is substituted by

$$j_{c1}+j_{e1}-j_{i1}\sqrt{m_e/m_i}=j_{1R}, \tag{38}$$

where the constant $-j_{1R}$ is the net perturbation electric current traversing the core. Densities and velocities for the remaining five differential equations follow:

$$\begin{aligned}
&\frac{n_{i1}}{n_{i0}}=\frac{j_{i1}}{j_{i0}}-\frac{k_{i1}-\phi_1}{v_{i0}^2},\\
&\frac{n_{e1}}{n_{e0}}=\frac{v_{e0}^2 j_{e1}/j_{e0}-k_{e1}-\phi_1}{v_{e0}^2-3t_{e0}},\\
&\frac{n_{c1}}{n_{c0}}=\frac{k_{c1}+\phi_1}{t_{c0}},\\
&\frac{v_{i1}}{v_{i0}}=\frac{k_{i1}-\phi_1}{v_{i0}^2},\\
&\frac{v_{e1}}{v_{e0}}=\frac{k_{e1}+\phi_1-3t_{e0}j_{e1}/j_{e0}}{v_{e0}^2-3t_{e0}}.
\end{aligned} \tag{39}$$

Finally, the electric potential satisfies

$$\begin{aligned}
&\phi_1=\frac{q_1}{p_0},\quad p_0=\frac{n_{c0}}{t_{c0}}-\frac{n_{i0}}{v_{i0}^2}-\frac{n_{e0}}{v_{e0}^2-3t_{e0}},\\
&q_1=-\frac{n_{c0}}{t_{c0}}k_{c1}+n_{i0}\left(\frac{j_{i1}}{j_{i0}}-\frac{k_{i1}}{v_{i0}^2}\right)-\frac{n_{e0}v_{e0}^2}{v_{e0}^2-3t_{e0}}\left(\frac{j_{e1}}{j_{e0}}-\frac{k_{e1}}{v_{e0}^2}\right).
\end{aligned} \tag{40}$$

Notice that in the low frequency range, there were just two differential equations for the $i-e$ modes.

Seven boundary conditions are needed to integrate the core equations and determine ξ_{D1}. Since ϕ_1 is obtained from the quasineutrality equation (40), none of these conditions can fix ϕ_1 at any point. However, it seems natural to govern the perturbations of the electrostatic potential at the contactor surface, ϕ_{1R}. We discussed already this issue in Ref. 2, and we concluded that a perturbation sheath tied to the quasineutral core is formed to accommodate ϕ_{1R} to the potential at the inner end of the core (the sheath is region *RN* in Fig. 3). Thus, here we impose the following eight conditions.

(i)–(ii) The DL conditions (17)–(18) on species e yield

$$[j_{e1}/j_{e0}+i\omega_e\xi_{D1}/v_{e0}]_{\xi_{D0}^-}^{\xi_{D0}^+}=0, \tag{41}$$

$$[k_{e1}+i\omega_e v_{e0}\xi_{D1}]_{\xi_{D0}^-}^{\xi_{D0}^+}=0, \tag{42}$$

with $j_{e1D}^+(j_{1\infty})$ and $k_{e1D}^+(j_{1\infty})$, and $\xi_{D1}(j_{1\infty})$ given by the presheath solution.

(iii) Since the DL is a barrier for species c, its total perturbation flow is zero,

$$[j_{c1}/n_{c0}\xi^2]_{\xi_{D0}^-}+i\omega_e\xi_{D1}=0. \tag{43}$$

(iv) The Langmuir condition (19) is satisfied.

(v) At high frequencies, the perturbation of the emitted ion current is zero, $j_{i1}(1)\simeq 0$.

(vi) Since $\xi=1$ is a singular point of the stationary solution, we have $p_0(1)=0$. Then, for ϕ_1, Eq. (40), to be bounded around $\xi=1$, we impose

$$q_1(1)=0. \tag{44}$$

(vii) ϕ_{1R} is known.

(viii) $k_{c1R}\equiv\phi_{1R}+t_{c0}n_{c1R}/n_{c0R}$ is known.

To impose the pair $(\phi_{1R},\ k_{c1R})$ is equivalent to give the more natural pair $(\phi_{1R},\ n_{c1R})$. No condition on j_{c1} is imposed at $\xi=1$ since we impose already condition (iii) on j_{c1}.

Since $q_1(1)=0$, the quasineutral potential at point N is obtained from applying l'Hopital rule to Eq. (40), that is

$$\phi_{1N}=\lim_{\xi\to 1} q_1/p_0.$$

When this value is different from ϕ_{1R}, the perturbation sheath accommodates the potential difference $\phi_{1N}-\phi_{1R}$. In the zero Debye-length limit, Eqs. (20) and (21) yield

$$k_{\alpha 1N}=k_{\alpha 1R},\quad j_{\alpha 1N}=j_{\alpha 1R},$$

and the jumps of $n_{\alpha 1}$ and $v_{\alpha 1}$ from points R to N are determined from these conservation conditions and the potential jump. We do not need to know the internal structure of the sheath to solve the quasineutral problem.

Once the preceding conditions are applied, the general solution of the core equations between points N and D^- relate magnitudes at D^- to the perturbation parameter k_{c1R} in the form

$$[j_{i1D}^-\ \ k_{i1D}^-\ \ \xi_{D1}]A=k_{c1R}B, \tag{45}$$

for certain matrices A and B, which depend on ω_e and the zeroth-order solution. Therefore, leaving apart ϕ_{1R}, which modifies the perturbation sheath *RN* exclusively, the perturbation response of the whole structure depends only on k_{c1R} and ω_e.

Temporal eigenmodes of the perturbation problem correspond to nontrivial solutions for $k_{c1R}=0$. These eigenmodes exist for those stationary solutions making matrix A, in Eq. (45), singular. Thus, the dispersion equation of the complete plasma structure is

$$D(\omega_e;j_{i0},\phi_{0R},t_{c0},m_e/m_i)=0, \tag{46}$$

with $D=\det A$.

B. Cases $\omega_i\gg 1$ and $\omega_i=\infty$

For $|\omega_i|\gg 1$ [and $\omega_e=O(1)$] the core equations admit a WKB solution too. As in the presheath case, the WKB solution is similar to the one obtained in Ref. 2 except for it includes the effect of $\omega_e\neq 0$. It consists of one pair of short-wavelength, $i-e$ modes (moving with the i beam) and two pairs of $e-e$ modes.

For $|\omega_i|\to\infty$ that WKB solution justifies to assume the i population as quasirigid.[19] We take

$$n_{i1}(\xi)=0,\quad v_{i1}(\xi)=0, \tag{47}$$

and keep the four differential equations for the $e-e$ modes. Using Eq. (47) in Eq. (40), the electrostatic potential satisfies

$$\left(\frac{n_{c0}}{t_{c0}}-\frac{n_{e0}}{v_{e0}^2-3t_{e0}}\right)\phi_1$$

$$\simeq -\frac{n_{c0}}{t_{c0}}k_{c1}-\frac{n_{e0}}{v_{e0}^2-3t_{e0}}\left(v_{e0}^2\frac{j_{e1}}{j_{e0}}-k_{e1}\right). \quad (48)$$

Notice that the indeterminacy of $\phi_1=q_1/p_0$ at $\xi=1$ has disappeared in Eq. (48) thanks to the substitution $k_{i1}=\phi_1$. Condition (44) can be omitted, but still the perturbation sheath *RN*, tied to the contactor, is needed to connect ϕ_{1R} to $\phi_{1N}=\phi_1(1)$, this last one coming out now from Eq. (48).

Since the DL becomes rigid for $\omega_i=\infty$, the conditions at point D^- simplify. In particular, we have

$$k_{e1D}^-=k_{e1D}^+, \quad j_{c1D}^-=0, \quad j_{e1D}^-=j_{e1D}^+, \quad (49)$$

with $k_{e1D}^+(j_{1\infty})$ and $j_{e1D}^+(j_{1\infty})$ given by Eq. (37) for the presheath. This yields

$$j_{1R}=j_{1\infty}, \quad (50)$$

for the perturbation currents in core and presheath. Finally, the relations $k_{c1D}^-(j_{1\infty})$ and $\phi_{1D}^-(j_{1\infty})$ are obtained from Eq. (48) and the Langmuir condition, which here simplifies to

$$(1-v_{i0D}^-/v_{i0D}^+)n_{i0D}^-\phi_{1D}^-+n_{c0D}^-k_{c1D}^-+n_{e0D}^-k_{e1D}^-$$
$$+(v_{e0D}^--2v_{e0D}^+)j_{1\infty}/\xi_{D0}^2=0. \quad (51)$$

Therefore, the core equations for the electrons can be integrated from ξ_{D0}^- to the contactor surface using $j_{1\infty}$ as the unique free parameter. This implies that the matrix relation (45) reduces here to the scalar relation

$$D(\omega_e;j_{i0},\phi_{0R},t_{c0}) \;\; j_{1\infty}=k_{c1R}, \quad (52)$$

which yields directly a function D for the dispersion relation (46).

C. Case $|\omega_e|\gg 1$

This asymptotic limit allows us to obtain a WKB-type solution on ω_e for the core region. This solution is of interest to understand the characteristics of the $e-e$ modes and their mutual interaction, and to obtain a semianalytical expression for the dispersion relation. The general form of the asymptotic solution can be found in Ref. 19. Here, we write down the WKB solution only for cases where

$$3t_{e0}/(v_{e0}^2-t_{c0})\ll n_{e0}/n_{i0}\ll 1,$$

which correspond to very large contactor potentials and moderate cores. For these cases, the WKB solution presents relatively simple expressions and retains still its main properties. The WKB solution is

$$j_{e1}(\xi)\simeq -\frac{\alpha(\xi)}{j_{e0}}(C_3\exp[i\omega_e\beta_+(\xi)]-C_4\exp[i\omega_e\beta_-(\xi)]),$$

$$k_{e1}(\xi)\simeq -\frac{i}{\alpha(\xi)}(C_3\exp[i\omega_e\beta_+(\xi)]+C_4\exp[i\omega_e\beta_-(\xi)])$$
$$+C_1+C_2\gamma(\xi), \quad (53)$$

$$\phi_1(\xi)=-k_{c1}(\xi)\simeq\frac{v_{e0}}{\xi^2 n_{c0}}j_{e1}(\xi)-C_1-C_2\gamma(\xi),$$

with

$$\alpha(\xi)=\xi^2 n_{e0}^{3/4}n_{c0}^{1/4},$$

$$\beta_\pm(\xi)=\int_{\xi_{D0}}^{\xi}\left(1\mp i\sqrt{\frac{n_{e0}}{n_{c0}}}\right)\frac{d\xi}{v_{e0}},$$

$$\gamma(\xi)=\int_{\xi_{D0}}^{\xi}\frac{d\xi}{n_{i0}\xi^2}.$$

Equations (37) and (49) state that $k_{e1D}^-=k_{e1D}^+=c_p i\omega_e j_{1\infty}\gg j_{1\infty}$. Making the ansatz

$$k_{e1},k_{c1},\phi_1,C_l=O(\omega_e)j_{1\infty} \quad (l=1,2,3,4),$$

$$C_3-C_4\ll O(\omega_e)j_{1\infty},$$

we have that, up to dominant order, the Langmuir condition (51) reduces to

$$k_{c1D}^-\simeq\frac{n_{e0D}^-}{n_{e0D}^--n_{i0D}^+}k_{e1D}^+,$$

and the integration constants in Eq. (53) satisfy

$$C_2\simeq i\omega_e j_{1\infty}, \quad C_1\simeq k_{c1D}^-,$$

$$C_3\simeq C_4\simeq -\frac{i\alpha_D^-}{2}\frac{n_{i0D}^+}{n_{e0D}^--n_{i0D}^+}k_{e1D}^+.$$

The WKB solution (53) shows that, of the four $e-e$ modes, those proportional to C_1 and C_2 are related to the c population and are stationary (in time) in the laboratory frame. Those proportional to C_3 and C_4 are related to the e population and form a pair which is stationary in the e-beam frame; of this last pair, each individual mode grows spatially in a different direction. The condition $C_3\simeq C_4$, together with $\beta_+(\xi_{D0})=\beta_-(\xi_{D0})=0$ implies that the mode growing inwards is dominant always; for $\mathrm{Re}(\omega_e)>0$ this mode corresponds to $\beta_+(\xi)$.

To close the problem we set $k_{c1}(1)=k_{c1R}$ in Eq. (53). This yields an analytical expression for function D in Eq. (52),

$$\frac{D}{\omega_e}\simeq\left(\frac{\alpha_D^-}{2n_{e0R}^{1/4}n_{c0R}^{3/4}}\exp[i\omega_e\beta_+(1)]n_{i0D}^++in_{e0D}^-\right)$$
$$\times\frac{c_p}{n_{e0D}^--n_{i0D}^+}+i\gamma(1). \quad (54)$$

V. REGULAR RESPONSE

Figure 5 shows the space-temporal response of the electric potential, $\Phi(r,t)=\Phi_0(r)+\Phi_1(r,t)$, for two cases of purely oscillatory perturbations of the density n_{c1R}. In the core, we observe that, at low ω_e, the modes which are stationary in the laboratory frame dominate over the pair of modes moving with the e beam; on the contrary at high ω_e, the mode moving with the e beam and growing inwards becomes the dominant one. At the presheath the stationary wave dominates over the $i-e$ mode. The discontinuity observed at $r=R$ corresponds to the small sheath adjusting $\phi_{1N}\simeq -k_{c1R}$ to $\phi_{1R}=0$.

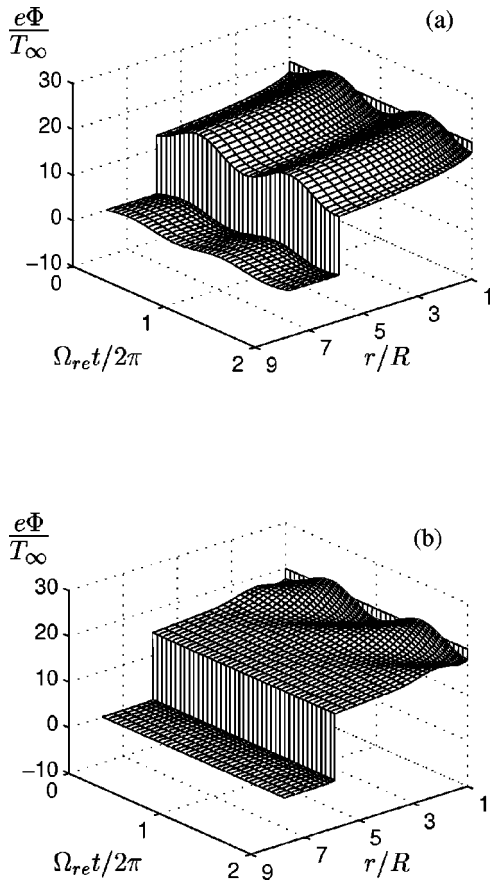

FIG. 5. Complete regular response of the electrostatic potential to perturbations at $r=R$ characterized by $k_{c1R}/\phi_{0R}=0.1$, $\phi_{1R}=0$, $\omega_i=\infty$, and $\omega_e=1$ (a), 10 (b). The stationary solution corresponds to $\phi_{0R}=20$, $\xi_{D0}=5.89$, and $t_{c0}=1$.

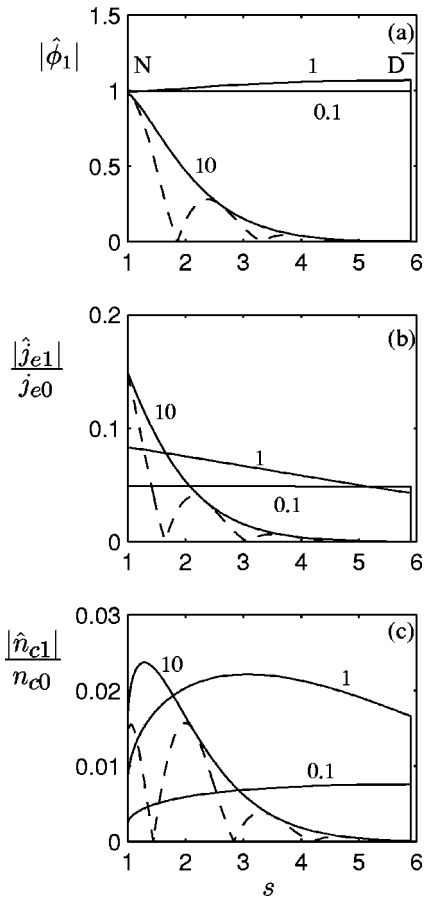

FIG. 6. Envelope of the spatial response to perturbations charcterized by $k_{c1R}\neq 0$ and $\omega_e=0.1$, 1, and 10. Amplitudes are normalized with $k_{c1R}=1$. The dashed lines are the instantaneous profiles for $\omega_e=10$. The stationary solution corresponds to $\phi_{0R}=20$, $\xi_{D0}=5.89$, and $t_{c0}=1$. Given ϕ_{1R}, the sheath (discontinuity) RN adjusts the difference $\phi_{1N}-\phi_{1R}$.

Figure 6 shows the spatial envelope [without the dependence on $\exp(-i\Omega t)$] of different perturbation variables for $n_{c1R}\neq 0$, $\phi_{1R}=0$, and different frequencies. We observe that the perturbation sheath RN transmits most of the perturbation of n_{c1R} to ϕ_{1N}. As a consequence, the most perturbed magnitude in the core is ϕ_1. The perturbation ϕ_{1N} is transmitted along the core by the modes related to species c. The interaction with the DL produces the perturbation $j_{1\infty}$ which is transmitted both toward the contactor, by one of the modes related to species e, and outwards, along the presheath. The different dominant modes at each distinguished range of ω_e explain that, for ω_e small, the spatial envelope is practically constant along the core (these solutions are similar to those of Ref. 2) whereas, for ω_e large, the amplitude of the perturbation increases toward the contactor. The relative magnitudes of the perturbations in the core follow $n_{e1}/n_{e0}\sim j_{e1}/j_{e0}\sim j_{c1}/j_{e0}\sim\phi_1/v_{e0}^2$.

VI. INSTABILITY MODES

We discuss here the unstable eigenmodes of the whole plasma structure. We present results for the asymptotic limit $\omega_i=\infty$, when the DL displacement, $\xi_{D1}=0$, can be neglected. For each stationary plasma structure, the eigenfrequencies are the solutions of the dispersion relation (46). These solutions can be expressed as

$$\omega_e^n=\omega_e^n(\xi_{D0},\phi_{0R},t_{c0}),\quad n=1,2,\ldots,$$

where each n indicates a particular family of harmonics. Eigenmodes are nontrivial solutions for homogeneous boundary conditions at the contactor surface, i.e., $n_{c1R}=\phi_{1R}=0$. In particular, eigenmodes develop perturbations of the net current. Thus, $j_{1\infty}$ is a convenient parameter to measure the instability amplitude.

For the particular range $\omega_e\gg 1$, analytical expressions can be obtained from solving Eq. (54) for $\exp[i\omega_e\beta_+(1)]$. This yields

$$\beta_+(1)\omega_e^n\simeq(\tfrac{3}{2}+2n)\pi - i\ln\left(\frac{\gamma(1)(n_{e0D}^- - n_{i0D}^+)+c_p n_{e0D}^-}{c_p n_{i0D}^+\alpha_D^-}\,2n_{e0R}^{1/4}n_{c0R}^{3/4}\right),$$

and, for large n, it simplifies to

$$\omega_{e,re}^n\simeq 2\pi n|v_{e0}|/(\xi_{D0}-1),\quad \omega_{e,im}^n\simeq\omega_{e,re}^n\sqrt{n_{e0}/n_{c0}}. \tag{55}$$

Figure 7 shows the first three families of harmonics versus ξ_{D0}, for ϕ_{0R} and t_{c0} given. For each zeroth-order solution there is a countable family of unstable modes, with both

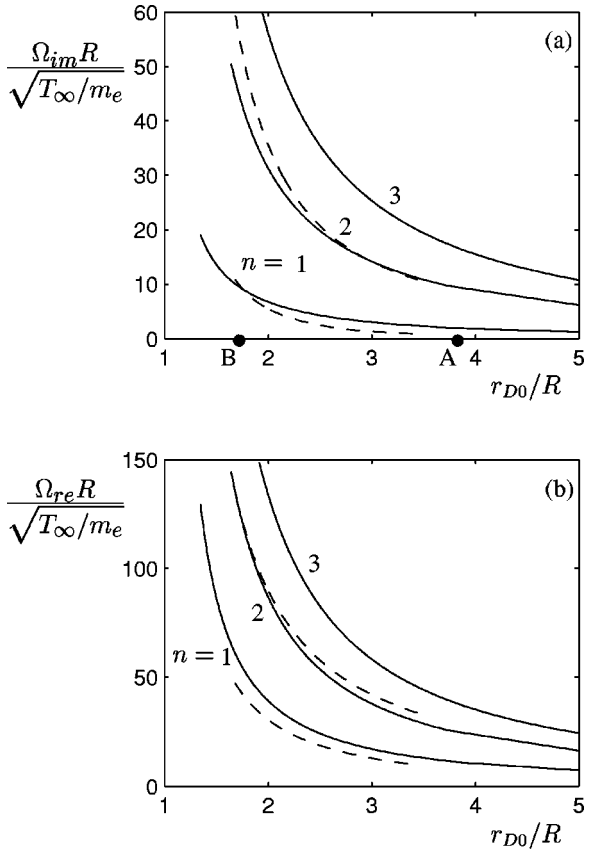

FIG. 7. Frequencies of eigenmodes $n=1$, 2, and 3 versus the core size. The dashed lines are the solutions of the approximate nonzero Debye-length model (of Sec. VI A) in the limit $\lambda_{D\infty}/R\to 0$. Other parameters are $\phi_{0R}=100$ and $t_{c0}=10$. Point *A* and *B* correspond to solutions shown in Figs. 8 and 10, respectively.

$\omega^n_{e,re}$ and $\omega^n_{e,im}$ growing with n. (Space-charge effects, to be treated in the next subsection, limit the number of unstable modes and the maximum value of $\omega_{e,im}$.) Figure 8 shows space–temporal profiles of the first three unstable modes for a particular stationary solution (point *A* in Fig. 7). The mode traveling with the *e* beam and growing from the DL to the contactor provides the main contribution to the eigenmode. The spatial wavelength of the instability depends on both the core size and the harmonic number. This is confirmed by Fig. 9, which shows the spatial envelope for the eigenmode $n=2$ and two stationary solutions with different core sizes. In addition, Eq. (55) shows that the spatial wavelength is related directly to ω_{re}. The amplitudes of the eigenmodes in the presheath are negligible; the presheath just provides the convenient conservation and jump conditions at the external side of the DL and transmits the perturbation of the current outwards.

A. Space-charge effects and maximum growth rate

The high-frequency eigenmodes correspond to a reactive electron–electron instability. The main characteristics of this instability in a three species plasma were discussed in Ref. 16 for the basic case of a semiinfinite, planar plasma. The unbounded character of the family $\omega^n_{e,im}$ for a particular stationary solution is related to the zero Debye-length limit of

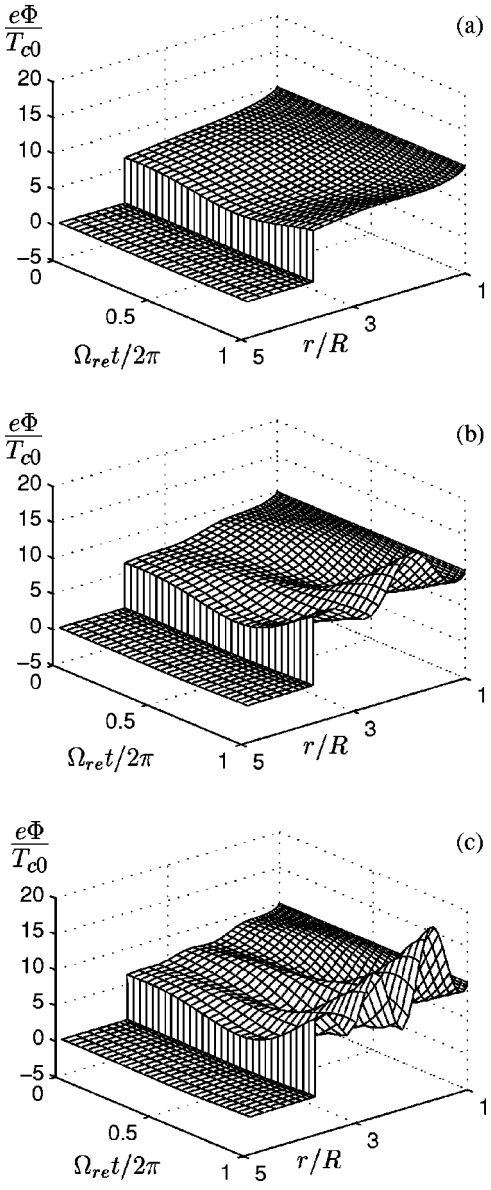

FIG. 8. Space-temporal evolution of $\Phi(r,t)$ for the first three eigenmodes, $n=1$ (a), 2 (b), and 3 (c). The stationary solution corresponds to $\phi_{0R}=100$, $\xi_{D0}=3.716$, and $t_{c0}=10$.

the present perturbation model. It is known that the reactive $e-e$ instability is bounded by space-charge effects or, to be more precise, by the coupling of the unstable $e-e$ modes with non-neutral Langmuir modes, of much shorter wavelength.[17]

Therefore, this perturbation model is correct only for modes with wavelengths satisfying $\lambda=R|v_{e0}/\omega_e|\gg\lambda_d$, where λ_d is the typical Debye length in the core. In order to determine the most unstable mode, space-charge effects must be included in core and presheath, which means to replace the quasineutrality condition by the full Poisson equation,

$$\frac{\lambda^2_{D\infty}}{R^2}\frac{1}{\xi^2}\frac{d}{d\xi}\left(\xi^2\frac{d\phi_1}{d\xi}\right)=n_{e1}+n_{c1}-n_{i1}-n_{a1}.$$

An exact solution of the resulting problem is difficult to obtain because of the disparity of spatial scales involved, the coupling with the non-neutral DL, and the inhomogeneity of

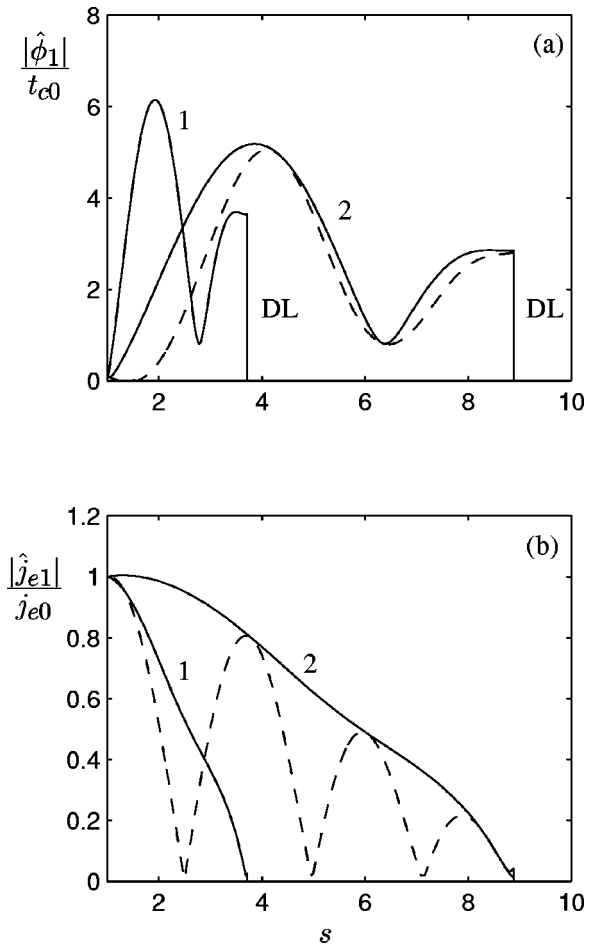

FIG. 9. Profiles of the eigenmode $n=2$ for two core sizes, $\xi_{D0}=3.716$ (1) and 8.883 (2). The dashed line represents an instantaneous profile for $\xi_{D0}=8.883$. Other parameters are $\phi_{0R}=100$ and $t_{c0}=10$.

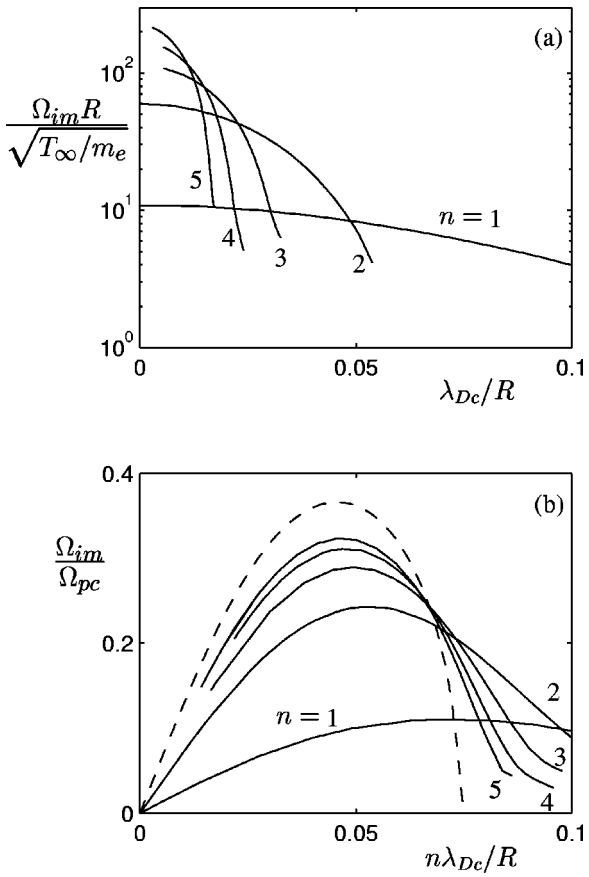

FIG. 10. Influence of a nonzero Debye-length on the instability growth rate. The dashed line in (b) corresponds to $\Omega_{im}(\kappa)$ of the eigenmodes of an infinite plasma for $\kappa=(3\pi/2)(r_{D0}-R)^{-1}n$. The stationary solution corresponds to $\phi_{0R}=100$, $\xi_{D0}=1.68$, and $t_{c0}=10$.

the stationary solution. Here, an approximate analysis is carried out, aimed mainly to confirm the stabilizing effect of the Langmuir modes and to estimate which is the most unstable mode in terms of $\lambda_{D\infty}/R$ and the rest of parameters of the stationary solution.

The approximate treatment of the problem (for $\omega_i=\infty$) is based on the following assumptions. First, in the presheath, which is practically unaffected by modes with $\omega_e \gg 1$, we just take the solution leading to Eq. (37). Second, in the perturbation equations of the core, Eqs. (20) and (21), we replace the zeroth-order magnitudes (v_{e0}, n_{e0}, . . .) by average values and neglect spherical effects (i.e., $2/\xi \ll d/d\xi$). The fluid and Poisson equations are then integrated analytically for each ω_e. The general solution (in the core) is the combination of six fundamental modes,

$$Y(\xi)=b_1+b_2\xi+\sum_{j=3}^{6} b_j \exp(\tilde{\kappa}_j\xi),$$

with $\tilde{\kappa}_j \equiv \kappa_j(\Omega)R$, and κ_j the solutions of the dispersion relation

$$\frac{\Omega_{pc}^2}{\Omega^2-\kappa^2C_c^2}+\frac{\Omega_{pe}^2}{(\Omega-\kappa V_{e0})^2-\kappa^2C_e^2}=1,$$

with $\Omega_{p\alpha}^2=e^2N_\alpha/\epsilon_0 m_e$ and $C_\alpha^2=\rho_\alpha T_{\alpha 0}/m_\alpha$. Finally, to determine $j_{1\infty}$ and the constants b_j ($j=1,..,6$) we apply the five boundary conditions on the $e-e$ modes plus two conditions on the electrostatic potential. Clearly, one of these two conditions is $\phi_{1R}=0$ (and the perturbation sheath *RN* is part now of the core solution). For the second condition on ϕ_1 we take

$$\lambda_{D\infty}[d\phi_1/d\xi]_{\xi_{D0}^-}\simeq 0,$$

which is correct while the space-charge effects are much smaller in the core side than in the DL one. (In any case, we have verified that the replacement of this condition with a linear combination of the form $[a\phi_1+b\,d\phi_1/d\xi]_{\xi_{D0}^-}=0$, for certain constants a and b, does not modify the conclusions to come.[19]) To check the validity of this approximate model, Fig. 7 compares, for the limit $\lambda_{D\infty}/R=0$, the frequencies of two singular modes obtained from the approximate and the exact models. The agreement is good enough to accept the qualitative conclusions of the approximate model.

Figure 10(a) presents solutions of the approximate perturbation model for nonzero Debye length. It shows the evolution of $\omega_{e,im}^n$ with λ_{Dc}/R for the families $n=1,\ldots,5$; for convenience, $\lambda_{Dc}=\lambda_{D\infty}\sqrt{N_\infty/N_{c0}}$ is used instead of $\lambda_{D\infty}$. We observe that nonzero λ_{Dc}/R has a stabilizing effect over all eigenmodes, which is more pronounced the larger is n. As

a consequence, the index n of the most unstable mode tends to decrease with λ_{Dc}/R increasing, and for $\lambda_{Dc}/R>0.01$ (and the stationary solution used in Fig. 10) the most unstable mode corresponds already to $n=1$.

B. Finite-size effects

The $e-e$ instability in our plasma structure develops mainly in the core. Therefore, it must be influenced by the finite size of this region and the conditions at the boundaries, mainly at the DL. Then, a subject of interest is the relation of this $e-e$ instability with the eigenmodes of the $e-e$ instability developing in a similar but infinite and homogeneous plasma. The instability type for this basic case (and similar plasma conditions) is the *reactive, weak-beam* instability.[17,20] This presents a continuous family of eigenmodes (of wave number κ) and the (local) dispersion relation yields Ω_{im}/Ω_{pc} in terms of $\kappa\lambda_{Dc}$ and the parameters of the zeroth-order solution. The maximum growth-rate and wave number of the weak-beam instability satisfy

$$\Omega_{im}/\Omega_{pc}\simeq 3^{1/2}2^{-4/3}(N_{e0}/N_{c0})^{1/3},\quad \kappa/\lambda_{Dc}=C_c/V_e. \qquad (56)$$

The comparison of the two problems requires to relate the wave number κ and the index n, characterizing the eigenmodes of each problem. Taking into account that the wavelength of the eigenmodes of our spherical structure decrease with n or $(r_{D0}-R)^{-1}$ increasing, Fig. 10(b) presents that comparison for the data of Fig. 10(a) and $\kappa=(3\pi/2)\times(r_{D0}-R)^{-1}n$, where the numerical factor was adjusted for a good fit at large n. The close relation between the two problems is clearly observed. As it is reasonable, short-wavelength harmonics (that is, those with large n) are less affected by finite-size effects and approach the basic instability properties, Eq. (56). At the other end, for $n=1$, the maximum growth rate is only one-third of the maximum of Ω_{im}. Finally, the parts of the solid lines, in Fig. 10(b), to the right of the dashed line (i.e., for $n\lambda_{Dc}/R$ large) indicate only that the selected relation between κ and n is incorrect there.

C. Instability threshold

The preceding analysis suggests that the fundamental eigenmode (i.e., $n=1$) characterizes the $e-e$ instability behavior when λ_{Dc}/R is not very small ($\lambda_{Dc}/R>0.01$ for the case of Fig. 10). In addition, $\omega^1_{e,im}$ is maximum for $\lambda_{Dc}=0$ and decreases slowly with λ_{Dc}. Therefore we expect the behavior of $\omega^1_{e,im}$ for $\lambda_{Dc}=0$ (which can be studied with the quasineutral perturbation model) to give a correct picture of the behavior of the dominant growth rate of the instability when λ_{Dc}/R is not very small.

Figures 11(a) and 11(b) show the evolution of $\omega^1_{e,im}$ with the contactor potential and the temperature ratio, for a given core size. The growth rate decreases when Φ_{0R}/T_{c0} or T_{c0}/T_∞ decrease, and the plasma becomes stable eventually. Figure 12 shows the stability threshold in the parametric plane (ϕ_{0R},ξ_{D0}) for two different values of T_∞/T_{c0}. For T_{c0} given, the stability of the plasma structure is favored by low Φ_{0R}, large T_∞, and large r_{D0}/R. Physically, this corresponds to a less supersonic e beam in the core.

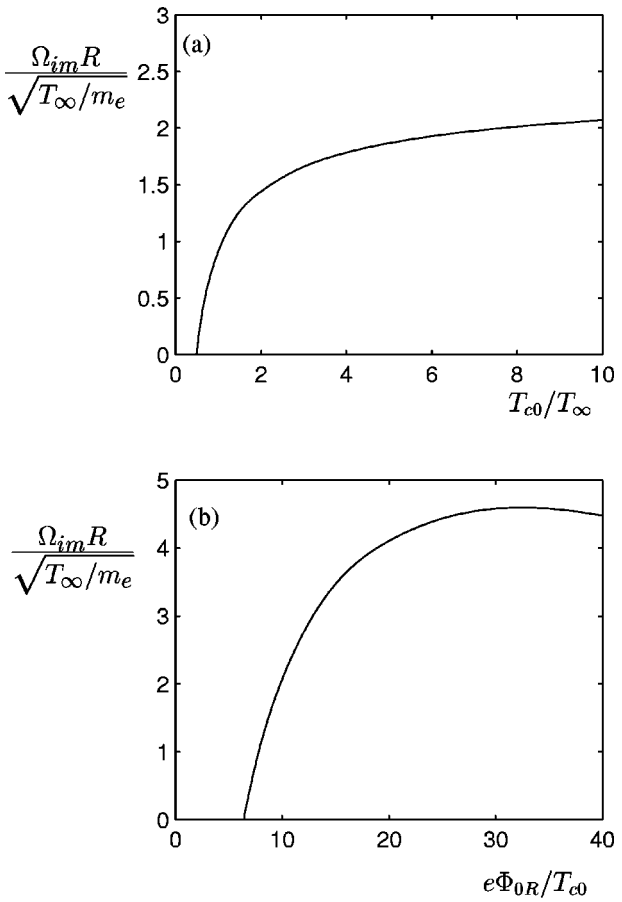

FIG. 11. Influence of the stationary solution on the growth rate of the fundamental mode for $\lambda_{Dc}/R=0$ (using the zero Debye-length model). In (a) $\phi_{0R}/t_{c0}=10$ and $\xi_{D0}=3.716$; in (b) $t_{c0}=10$ and $\xi_{D0}=3.716$.

We compare now our results with two experimental observations of contactor plumes with an intermediate DL. Vannaroni *et al.*[8] detected thermalization of the e beam in the core and propose the bump-in-tail instability as the probable cause (the bump-in-tail instability is the resistive case of the reactive weak-beam instability[17]). Williams and Wilbur[7] detected fluctuations of different amplitudes and frequencies,

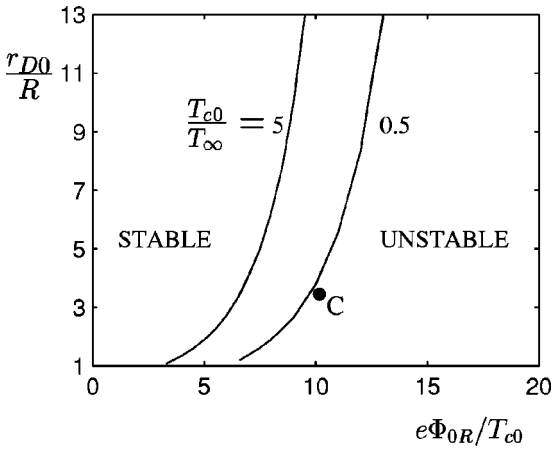

FIG. 12. Parametric regions of stability of the fundamental mode for $\lambda_{Dc}/R=0$ (using the zero Debye-length model) and two different temperature ratios. Point C corresponds to the case of Fig. 11(a).

but did not report any clear sign of an $e-e$ instability. The plasma structure of Vannaroni *et al.* is characterized by $t_{c0}=2$, $\xi_{D0}\simeq 3.8$, $\phi_{0R}/t_{c0}\simeq 13$, and $\lambda_{Dc}/R\sim 10^{-3}-10^{-2}$; for these values, our model predicts the presence of the reactive $e-e$ instability, controlled by an eigenmode with $n>1$. On the contrary, the plasma structure of Williams and Wilbur has $t_{c0}=0.33$, $\xi_{D0}\simeq 6.6$, $\phi_{0R}/t_{c0}=18$, and $\lambda_{Dc}/R\sim 0.02-0.1$, which is around the instability threshold of our model. Notice that stabilization by space-charge effects is much stronger in this second case. Therefore, as far as we can check, our model conclusions seem to agree with experimental observations.

VII. CONCLUSIONS

This paper extends to the high-frequency range the analysis of the nonstationary response of a spherical structure made up of two plasmas with an intermediate, strong DL. In contrast to the low-frequency range, the response is now characterized by (a) a more complex dynamic response, governed by traveling and stationary $e-e$ modes, (b) a negligible response of the ions, except for some boundary layers, (c) a negligible displacement of the DL, as a consequence of the ion behavior, and (d) the development of a reactive $e-e$ instability, launched by the supersonic electronic beam traversing the core. (The rigidity of the DL to high frequency perturbations would agree with the observation made by Joyce and Hubbard[12] that, in contrast to the $i-e$ instability, the $e-e$ instability does not disrupt the double layer itself.)

In the high-frequency range, the quasineutral perturbations in the presheath consist of the superposition of a stationary wave and a wave traveling outwards, plus an ion boundary layer close to the DL boundary. The presheath response is proportional to the net perturbation current, $j_{1\infty}$. The quasineutral response in the core consists of four waves, two are stationary in the laboratory frame, the other two are stationary (in time) in the frame of the inward e beam; each wave from this last pair grows spatially in a different direction. In addition, to adjust the perturbations of the electrostatic potential, there is a perturbation Debye sheath close to the contactor surface. The mechanisms of transmission of the perturbations along the different regions have been explained. The dominant electron modes are different for the cases $\omega_e=O(1)$ and $\omega_e\gg 1$.

The quasineutral perturbation model predicts the development of a reactive (i.e., macro) $e-e$ instability with a countable family of eigenmodes. However, a quasineutral model is unable to determine correctly the maximum growth rate (and the related eigenmode). An approximate perturbation model with space-charge effects was analyzed to solve that problem. Space-charge effects show that some of the previous stationary waves are indeed Langmuir modes, and the coupling of these modes with the $e-e$ ones bounds the instability. It is found that, except for very small Debye lengths, the fundamental eigenmode dominates the instability. Growth rates and other characteristics of the eigenmodes are consistent with the basic theory in an homogeneous, infinite plasma. Finite-size effects are found to modify mildly the growth rates of the eigenmodes.

For the cases when the fundamental mode dominates the instability, the parametric regions of stability (of the whole plasma structure) were investigated. The reactive instability tends to disappear for low contactor potentials, high temperatures of the ambient plasma, and large core sizes. The comparison of our results with two experiments on contactor plumes is satisfactory.

Finally, it must be pointed out that the disappearance of the reactive $e-e$ instability would leave still a weaker, resistive $e-e$ instability, due to the Landau resonance. Also, the ion beam crossing hypersonically the presheath can develop a weak $i-e$ instability at the presheath. Reference 17 provides estimates of the growth rates and other properties of these weaker instabilities.

ACKNOWLEDGMENT

This research was supported by the Ministerio de Ciencia y Tecnología of Spain under Project No. BFM-2001-2352.

[1] E. Ahedo and V. Lapuerta, Phys. Plasmas **2**, 3252 (1995).
[2] V. Lapuerta and E. Ahedo, Phys. Plasmas **7**, 2693 (2000).
[3] E. Ahedo, J. Sanmartín, and M. Martínez-Sánchez, Phys. Fluids B **4**, 3847 (1992).
[4] N. Hershkowitz, Space Sci. Rev. **41**, 351 (1985).
[5] M. A. Raadu, Phys. Rep. **178**, 26 (1989).
[6] R. Schrittwieser, *Double Layers and other Nonlinear Potential Structures in Plasmas* (McGraw-Hill, Singapore, 1992).
[7] J. Williams and P. J. Wilbur, J. Spacecr. Rockets **27**, 634 (1990).
[8] G. Vannaroni, M. Dobrowolny, E. Melchioni, F. de Venuto, and R. Giovi, J. Appl. Phys. **71**, 4709 (1992).
[9] P. Coakley and N. Hershkowitz, Phys. Fluids **22**, 1171 (1979).
[10] S. Torven and D. Anderson, J. Phys. D **12**, 717 (1979).
[11] M. Guyot and C. Hollestein, Phys. Fluids **26**, 1596 (1983).
[12] G. Joyce and R. Hubbard, J. Plasma Phys. **20**, 391 (1978); R. Hubbard and G. Joyce, J. Geophys. Res. **84**, 4297 (1979).
[13] C. K. Goertz and G. Joyce, Astrophys. Space Sci. **32**, 165 (1975).
[14] N. Singh and R. W. Schunk, J. Geophys. Res. **87**, 3561 (1982).
[15] T. Yamamoto, J. Plasma Phys. **34**, 271 (1985).
[16] V. Lapuerta and E. Ahedo, Phys. Plasmas **9**, 3236 (2002).
[17] V. Lapuerta and E. Ahedo, Phys. Plasmas **9**, 1513 (2002).
[18] C. M. Bender and S. A. Orszag, *Advanced Mathematical Methods for Scientists and Engineers* (McGraw-Hill, Singapore, 1986).
[19] V. Lapuerta, Ph.D. thesis, Universidad Politécnica de Madrid, Spain, 1999.
[20] D. B. Melrose, *Instabilities in Space and Laboratory Plasmas* (Cambridge University Press, Cambridge, 1986).